

## Resveratrol induced ER expansion and ER caspase-mediated apoptosis in human nasopharyngeal carcinoma cells

Shu-Er Chow · Cheng-Heng Kao · Yi-Tong Albert Liu · Mei-Ling Cheng ·  
Ya-Wen Yang · Yao-Kuan Huang · Chih-Chin Hsu · Jong-Shyan Wang

Published online: 22 November 2013

© Springer Science+Business Media New York 2013

**Abstract** Autophagy and endoplasmic reticulum (ER) stress response is important for cancer cells to maintain malignancy and resistance to therapy. *trans*-Resveratrol (RSV), a non-flavonoid agent, has been shown to induce apoptosis in human nasopharyngeal carcinoma (NPC) cells. In this study, the involvements of tumor-specific ER stress and autophagy in the RSV-mediated apoptosis were investigated. In addition to traditional autophagosomes, the images of transmission electron microscopy (TEM) indicated that RSV markedly induced larger, crescent-shaped vacuoles with single-layered membranes whose the expanded cisternae contains multi-lamellar membrane structures. Prolonged exposure to RSV induced a massive

accumulation of ER expansion. Using an EGFP-LC3B transfection and confocal laser microscopy approach, we found RSV-induced EGFP-LC3 puncta co-localized with ER-tracker red dye, implicating the involvement of LC3II in ER expansion. The proapoptotic effect of RSV was enhanced after suppression of autophagy by ATG7 siRNA or blocking the autophagic flux by bafilomycin A1, but that was not changed after targeted silence of IRE1 or CHOP by siRNA. Using caspase inhibitors, we demonstrated the upregulation of caspase-12 (casp12) and the activation of casp4 were associated with the proapoptotic induction of RSV through the caspase-9/caspase-3 pathway. Intriguingly, siRNA knockdown of casp12, but not caspase-4, decreased the susceptibility of the NPC cells to RSV-mediated apoptosis. Further, we showed that RSV dose-dependently increased the ceramide accumulation as assessed by LC-MS/MS system. Using serine palmitoyl-transferase (SPT, a key enzyme of de novo ceramide biosynthesis) inhibitors (L-cycloserine and myriocin), we found the increased ceramide accumulation was strongly correlated with the proapoptotic potential of RSV. This study revealed the ER expansion and upregulation of ER casp12 together may indicate profound biological effects of RSV and contributed to NPC cell death. Targeting the different status of ER stress may provide a possible strategy for cancer treatments.

S.-E. Chow (✉) · C.-H. Kao · Y.-W. Yang · Y.-K. Huang  
Department of Nature Science Center for General Studies,  
Chang Gung University, Taoyuan, Taiwan  
e-mail: chowse@mail.cgu.edu.tw

S.-E. Chow · M.-L. Cheng · J.-S. Wang  
Healthy Aging Research Center, Chang Gung University,  
Taoyuan, Taiwan

Y.-T. A. Liu  
School of Medicine, University of New Mexico, Albuquerque,  
NM, USA

M.-L. Cheng  
Department of Biomedical Sciences, Chang Gung University,  
Taoyuan, Taiwan

C.-C. Hsu  
Department of Physical Medicine and Rehabilitation,  
Chang Gung Memorial Hospital, Keelung, Taiwan

J.-S. Wang  
Graduate Institute of Rehabilitation Science, Chang Gung  
University, Taoyuan, Taiwan

**Keywords** Resveratrol · ER expansion · Caspase-12 ·  
Apoptosis · NPC · Autophagy

### Introduction

The endoplasmic reticulum (ER) is a central organelle of lipid synthesis. It stores high intracellular calcium, and

allows protein folding as well as protein maturation. Disruption of any of these processes leads to ER stress. The intracellular signaling of unfolded protein response (UPR) is induced by ER stress often as a protective mechanism and initiates three primary ER-localized protein stress sensors: IRE1 $\alpha$  (inositol-requiring 1 alpha), PERK (double-strand RNA-activated protein kinase-like ER kinase) and ATF6 [1]. Cancer cells may adapt to ER stress and evade stress-induced apoptotic pathways by differentially activating the UPR branches [2]. The UPR might provide survival signaling pathways required for tumor growth. Increasing evidences suggest that increased expression of these UPR components as well as ER chaperones GRP78/BIP, GRP94, and GRP170 have been detected in many cancer cells such as breast cancer, hepatocellular carcinomas, gastric tumors, esophageal adenocarcinomas and more [2–4].

Autophagy is a lysosome-mediated intracellular degradation system characterized by the formation of double-membraned autophagosomes. It plays an important role in a variety of biological processes, including cell death, development and cancer [5]. As a dynamic and highly inducible catabolic process that responds to external cues, autophagy acts non-selectively on the turnover of long-lived proteins and damaged organelles or selectively targets distinct organelles (such as the ER in ER-phagy) [6], to remodel cell function. Autophagic flux refers to the dynamic process of autophagosome synthesis and degradation of autophagic substrates inside the lysosome, denoting a complete process of autophagy [5]. A set of autophagy-related (ATG) proteins (such as ATG5, ATG6 etc.) is hierarchically recruited to the phagophore, the initial membrane template in the construction of the canonical autophagosome [7]. Recently, non-canonical pathways, which lead to autophagosomal degradation through variants of the canonical pathway, have been described where the formation of the double-membraned autophagosome may occur in the absence of some of the key autophagy proteins (such as Beclin1) [7]. This autophagosome is possibly derived from a pre-existing membrane (ER, plasma membrane, mitochondria or Golgi) [7]. Autophagy has been associated with the effect of various cytotoxic chemotherapeutic agents in cancer cells, having either pro-survival or pro-death effects. Thus, this alternative pathway might provide another therapeutic opportunity.

Recently, more and more researches has demonstrated that the UPR is an important mechanism required for cancer cells to maintain malignancy and therapy resistance [3, 4]. Under prolonged and severe ER stress, the UPR induces cell death programs to eliminate the stressed cells [1, 3]. Most importantly, the level of CHOP expression is elevated and may function to mediate the onset of ER stress-associated apoptosis [8]. Caspase-4 (casp4) and caspase-12 (casp12), members of the inflammatory caspase

family, are shown to contribute to amyloid- $\beta$  neurotoxicity and are specifically activated by ER stress from disruption of calcium homeostasis and accumulation of excess proteins in the ER [9–11]. Casp12-deficient mice are resistant to ER stress-induced apoptosis, suggesting its critical role in the proapoptotic process [12]. It has been shown that the full-length casp12 polymorphism is only present in certain sub-Saharan African populations (28 % of individuals) and casp4 substitutes for its function in other individuals [13]. However, recent findings indicate that the full-length casp12 could be re-expressed in human tissue under certain pathologic conditions, including proximal tubule of human kidney, cancers such as Hep-J5 [14, 15], and multiple myelomas [16]. In particular, casp12 is up-regulated in response to high glucose and albumin in human HK-2 cells [17]. siRNA silencing of human casp12 protects tubular cells from albumin-induced apoptosis [17]; thus, the presence of casp12 in human and the role of casp12 in ER stress-induced apoptosis both needed to be investigated.

*trans*-Resveratrol (RSV), a natural non-flavonoid drug, has been shown to prevent pathogenesis and/or slow down the progression of a variety of diseases ranging from cancer and metabolic disorders to premature aging [18]. Ceramide is a biologically active sphingolipid that induces apoptosis, among other forms of cell death, and triggers autophagy [19]. RSV has been shown to cause the accumulation of misfolded proteins and ceramide in the ER, inducing autophagy and ER stress-associated apoptosis in cancer cells [18, 20, 21]. Ceramide accumulation induced by RSV is traced to the activation of serine palmitoyltransferase (SPT), the key enzyme of de novo ceramide biosynthetic pathway [21]. Recently, RSV was found to promote WIPI1-dependent LC3 lipidation in the absence of induced phagophore formation, indicating that different membrane sites may be used during non-canonical autophagy [20]. However, the effect of RSV-mediated ceramide accumulation on the formation of autophagy and apoptosis is still unclear. In this study, the molecular mechanisms underlying RSV-mediated ER stress and ER stress-associated apoptosis were investigated. We found that RSV induced ER stress-mediated cell death was accompanied by ER expansion, autophagy induction, and the activation of ER-resided casp4 and casp12. However, these effects of RSV were counteracted by suppression of de novo ceramide biosynthesis. These findings suggest targeting the ER might be an effective strategy for cancer therapy.

## Materials and methods

### Cell culture and reagents

Human nasopharyngeal carcinoma cell lines NPC-TW076 and NPC-TW039 were isolated from different patients with

keratinized nasopharyngeal squamous cell carcinomas [22]. NPC cells were maintained in basal medium (DMEM/F-12 at 1:1 v/v; Invitrogen, 12,400-016) supplemented with 5–10 % fetal bovine serum in a humidified incubator at 37 °C, 5 % CO<sub>2</sub>. We purchased the following antibodies and chemicals: the caspase inhibitors were purchased from BioVision: Z-ATAD-fmk for casp12 (1079-100), Z-LEHD-fmk for casp9 (107420C) or Z-DEVD-fmk for casp3 (1143-1) and Z-LEVD-fmk for casp4 (1108-100). The antibody for casp4 was purchased from Santa-Cruz Biotechnology, sc-56056). The following antibodies were purchased from Cell Signaling, glyceraldehyde-3-phosphate dehydrogenase (2118), LC3B-I/II (2775), IRE1, ATF6 and p-PERK (9956), CHOP (5554), casp12 (9502), casp3 and cleaved casp3 (9665), casp9 (5554), PARP and cleaved PARP (9532). ER-Tracker Red dye was purchased from Invitrogen (E34250). All other chemicals were purchased from Sigma.

#### EGFP-LC3 transfection and ER-tracker studies

NPC cells were transfected with EGFP-LC3 plasmid (Addgene, Plasmid 11546) using Lipofectamine2000 reagent (Invitrogen, 11668-019) for 16 h. An ER-tracker incubation was performed on attached cells for confocal fluorescence, and live-cell images of ER after the cells were treated with RSV for 24 h were taken. The RSV-treated cells were co-labeled with ER-Tracker<sup>TM</sup> Red (BODIPY<sup>®</sup> TR Glibenclamide) (500 nM for 30 min at 37 °C). Glibenclamide (glyburide) binds to the sulphonylurea receptors of ATP-sensitive K<sup>+</sup> channels which are prominent on ER. The dye ER-tracker co-localized with EGFP-LC3, representing autophagy of ER components or a contribution of the ER to the autophagosome.

#### Microscopic images

Transmission electron microscopy (TEM) was utilized for analyzing the ultra-structural images of autophagosomes and ER expansion [23]. Trypsinized cells were fixed with 2.5 % glutaraldehyde in phosphate-buffered saline, followed by 2 % OsO<sub>4</sub>. After dehydration, thin sections (0.12 µm) were stained with uranyl acetate and lead citrate for observation under TEM. To assess the dilation of ER images after treatment with SPT inhibitor and RSV, thin sections (0.6 µm) were stained with toluidine blue for observation under light microscope (LM).

#### Apoptosis assay

Cell apoptosis was assayed by annexin V-Cy5 and PI staining (BioVision, K103-25) followed by FACS analysis. The cells were treated with RSV at the indicated concentrations for 24 h. The cells were pelleted and resuspended

in annexin V-binding buffer (10 mM HEPES, 150 mM NaCl, 5 mM KCl, 1 mM MgCl<sub>2</sub>, 1.8 mM CaCl<sub>2</sub>, pH 7.4) containing annexin V-Cy5 (1:1,000) and 1 mg ml<sup>-1</sup> PI. After incubation at room temperature for 5 min, the cells were analyzed with a FACS Calibur flow cytometer (Becton–Dickinson). The percentage of total apoptotic events was defined as the sum of the cells in the early stage (annexin V-Cy5 positive/PI negative) and late stage (annexin V-Cy5 positive/PI positive) of apoptosis as previously described [24].

#### Preparation of cell lysates and western blot analysis

The cells were seeded at a  $2 \times 10^5$  per 35-mm culture dish. The cells were incubated for 24 h and were pre-treated with caspase inhibitors, bafilomycin A1 for 2 h or siRNA, for 16 h prior to treatment with RSV for 24 h, the cells were washed with ice-cold phosphate-buffered saline and lysed in Mammalian Protein Extraction Reagent (Sigma, C2978). Protein samples (the same concentration per lane) were separated on a 10–12 % sodium dodecyl sulfate (SDS)-polyacrylamide gel and blotted onto polyvinylidene difluoride membranes, blocked in PBST (0.1 % triton in 1 × PBS) and probed with primary antibodies overnight at 4 °C. The membranes were then incubated with the appropriate horseradish peroxidase-conjugated secondary antibodies. The immunoreactive protein bands were developed by enhanced chemiluminescence. The immunoreactive bands were analyzed by a densitometer.

#### siRNA transfection

To explore the function of CHOP, IRE1, and casp12 in NPC076 and NPC039 cells, we used siRNA to silence their expression. The siRNA targeting IRE1 mRNA was designed and synthesized by Dharmacon Research Inc. (Lafayette, CO). The nontargeting siRNA (Ngi), 5'-UUCUCCGAAC-GUGUCACGU-3', served as the transfection-negative control. The siRNAs of ATG7, CHOP, casp12 and casp4 were purchased from Santa Cruz (sc-41447, sc-35437; sc-72797 and sc-72798). The transfection was performed using Lipofectamine2000 according to the manufacturer's protocol. The effectiveness of siRNA silencing was assayed by Western blot analysis.

#### Lipid extraction and UPLC–MS/MS analysis

For extraction of lipids, the NPC cells were suspended in ice-cold chloroform/methanol (2:1, v/v) solution and centrifuged at 700 × g for 20 min at 4 °C. The lower layer containing chloroform were collected, dried under nitrogen gas, and stored at –80 °C. Prior to ceramide analysis, the sample was dissolved in 200 µl of 40 % methanol. For

normalization the ceramide levels, a portion of the cell was used for protein measurement.

Liquid chromatographic separation was carried out on a 100 mm × 2.1 mm Acquity 1.7 μm UPLC CHS C18 column (Waters Corp; Milford, MA, USA) using a ACQUITY™ Ultra Performance Liquid Chromatography system (Waters, USA). Mass spectrometry was performed on a Waters Q TOFMS (SYNAPT G2S, Waters MS Technologies, Manchester, UK) operated in positive ion mode. C16 ceramide was served as a standard [25] and analyzed under identical chromatographic conditions with that of the profiling experiment. MS and MS/MS analyses were performed under the same conditions. MS/MS spectra were collected at 10 spectra per second, with a medium isolation window around 4 *m/z*. The relative level of ceramide was quantified using the area of C16 ceramide spike, and calculated as the relative percent of ceramide to the control group cells after doing normalization to the cellular proteins.

### Statistical analyses

Data are presented as mean ± SEM. The statistical differences were determined using Student–Newman–Keuls test and Dunn’s test (Sigma Stat Software Program, Jandel Scientific, San Rafael, CA). A *p* value of 0.05 or less was considered to be significant.

## Results

### RSV induced selective autophagy

To characterize the RSV-induced remodeling of the morphology, we carried out an ultrastructural analysis in a time-dependent manner (Fig. 1a–c, original magnification 8,000×). Autophagy is induced under a starvation status. To assess the variety of autophagy, NPC cell was under starvation overnight and incubated with or without RSV for different period as indicated. Control group cells were incubated in medium containing 1 % FBS, presenting a basal autophagy with autophagosome (AV) or autolysosome (AL) (Fig. 1a). In addition to traditional autophagosomes (usually 0.5–1.5 μm in diameter) [26] and autolysosomes formation, the RSV-treated cells were found to contain expanded vacuoles/cisternae of various shapes wrapped around the nucleus after a 7-h incubation period in medium containing 1 % FBS (Fig. 1b, I and II, white arrow). The enlarged cavity was still more or less continuous with each other and, especially of note, had expanded vacuoles presenting with crescent-like morphologies. This morphological characteristic suggests the induction of ER dilation. In particular, the lumen of some

of these crescent-like vacuoles (about 3.5–6 μm in long axis) was densely filled with the multi-lamellar membrane structure or the debris of organelle in the luminal space (Fig. 1b, I, and II, white arrow). The mitochondria (m) were clearly shown in the same treated condition (Fig. 1, I and III). Further, exposure to RSV for 24 h, a massive accumulation of expanded cisternae with pointy ends was shown in the sub-cellular compartment. Some of the crescent-like vacuoles formed large vacuoles containing degraded materials that seemed to be in the process of catabolic reaction (Fig. 1c). The TEM images also indicated that RSV induced an expansion of the ER and caused the formation of non-traditional autophagy associated with the ER membrane.

### RSV induced cell apoptosis accompanied with ER stress and autophagy

To examine the effect of RSV on ER stress, NPC cells were treated with RSV for different periods of time and the response of ER stress was assayed by the immunoblot of representative UPR markers. As shown in Fig. 2a, RSV induced marked increase of IRE1, p-PERK, and ATF-6α in a time-dependent manner. This induction of ER stress was confirmed by increased level of CHOP, a representative marker of ER stress, expression. RSV induced cell apoptosis accompanied by autophagy associated with both PARP cleavage and increased levels of LC3-II expression (Fig. 2b). Fold change amounts relative to the control, arbitrarily set to 1, are shown in the lower panel of Fig. 2a, b. The data indicated that RSV induced cell apoptosis associated with ER stress and autophagy.

To investigate whether RSV induced ER-phagy, a selective autophagy of the ER, NPC cells were transiently transfected with EGFP-LC3 for 24 h prior to incubation with RSV for 7 h, then stained with ER Tracker red and examined under confocal microscope. Figure 3 indicates RSV induced an increase in EGFP-LC3 puncta formation, indicating the lipidated LC3 induction. Interestingly, RSV induced an extensive co-localization of ER Tracker Red with EGFP-LC3 puncta (Fig. 3). The yellow fluorescence signal was markedly increased after overlaying the images of EGFP-LC3 and ER-tracker red dye. Taking the data of Figs. 1–3 together, RSV induction of the lipidation (puncta) of LC3 might be engaged in RSV-mediated dilation of the ER and/or the formation of ER-phagy. RSV treatment induced the lipidation of LC3, or the conversion of LC3-I to LC3-II. LC3-II may participate in ER expansion and could be an autophagy marker. It may also participate ER-phagy as LC3-II co-localized with ER-tracker Red dye and since the crescent vacuoles contain multi-lamella membrane structures and debris.

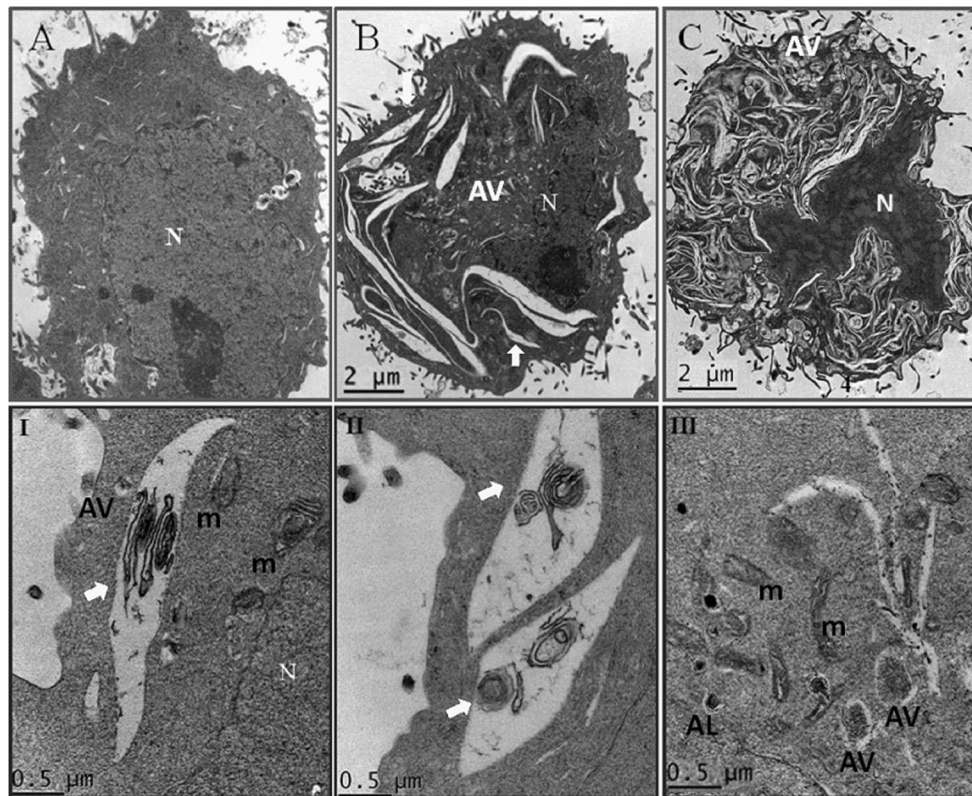


**Fig. 1** The morphology changes during the UPR induced by RSV. Electronic microscopy analysis of NPC cell exposed to 100  $\mu$ M RSV for the indicated times. **a–c** Magnified by  $\times 8,000$ . **I–III** High magnification images ( $\times 16,000$ ) of NPCs treated with RSV for 7 h. **I**, **II** Crescent-like vacuoles (3.5–6  $\mu$ m) with multi-lamella membranous

structures. **III** Autophagosomes (0.5–1.5  $\mu$ m), autolysosomes (with dense spots), and mitochondria with double-membranes. (White arrow crescent-like vacuole, N nucleus, m mitochondria, AV autophagosome, AL autolysosome.)

#### Silencing of ATG7 and suppression of autophagic flux enhanced RSV-mediated apoptosis

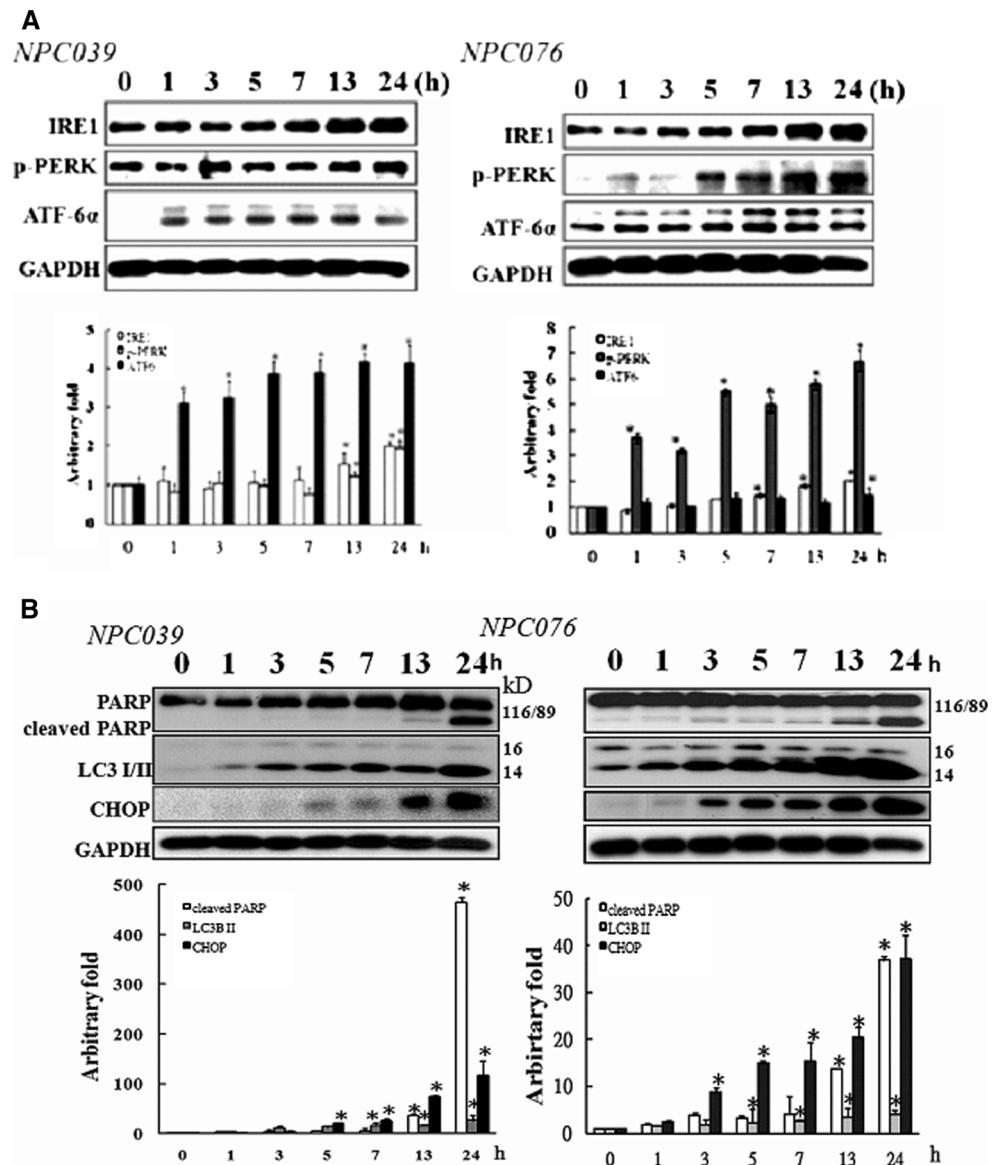
To assess the involvement of autophagy in RSV-induced cell death, NPCs were transfected with siRNA of ATG7, a key autophagy protein, to prevent the autophagy formation at an early stage. Targeted silencing of ATG7 effectively inhibited its expression (Fig. 4a, upper panel), and significantly enhanced RSV-mediated apoptosis as assessed by the annexin V positive cells (Fig. 4a, lower panel). Autophagic flux is crucial in determining whether the autophagosome fuses with the lysosome and is degraded or not [27]. Next, we investigated the effect on autophagic flux, a late stage of autophagy, the NPCs were incubated with bafilomycin A1 to suppress the fusion of autophagosomes and lysosomes. As shown in Fig. 4b, bafilomycin A1 markedly increased the levels of endogenous LC3-II, indicating the prevention of autophagic vacuole maturation. Simultaneously, bafilomycin A1 markedly enhanced the level of RSV-mediated LC3-II expression (Fig. 4b) and increased the sensitivity of NPC to RSV-mediated apoptosis that shown by increased annexin V-positive cells and

dose-dependent cleavage of PARP expression (Fig. 4b). Thus, the data clearly indicated autophagy plays a pivotal role in response to RSV.

Silence of IRE1 and CHOP expression did not change the RSV-mediated cell death

Several mechanisms have been proposed that link ER stress to apoptosis, including a direct activation of ER-associated caspases and CHOP, a common downstream pro-apoptotic molecule of UPR. First, we used siRNA technology to investigate the role of IRE1 and CHOP in response to RSV treatment. As shown in Fig. 5a, knock-down of IRE1 by its siRNA did not change the RSV-induced cell death, shown by the assay of annexin V-positive stained cells (Fig. 5a). Knock-down of CHOP effectively suppressed the levels of RSV-induced CHOP expression and did not affect RSV-induced apoptosis, shown by the annexin V-positive stained cells and PARP cleavage (Fig. 5b), suggesting the death effect induced by RSV was via a non-traditional apoptotic pathway.

**Fig. 2** RSV induced cell apoptosis accompanied with ER stress and autophagy induction. NPC cells were treated with RSV (100  $\mu$ M) for the indicated times. Cell lysates were analyzed for the levels of indicated proteins via Western blot. **a** The lysate was subjected to Western blotting to investigate the levels of the UPR markers IRE1, p-PERK, and ATF6 expression. **b** The lysate was subjected to Western blotting to investigate CHOP, PARP/cleaved PARP and LC3 I/II. GAPDH was shown as a loading control. Data shown represent three independent experiments and protein expression of each cell group was normalized to that of GAPDH. The *histograms* show arbitrary fold changes relative to the controls which were arbitrarily set at 1. \* $p < 0.05$  versus control group



Casp12 played a critical role in ER stress-induced NPC cell death

Next, the changes in the ER residents, casp12 and casp4, in response to RSV-mediated death were investigated. As shown in Fig. 6a, RSV induced significant up-regulation of casp12, as well as slight cleavage of casp4, associated with the cleavage of casp9 and casp3. Pre-treatment with the specific caspase inhibitors (Z-LEVD-fmk, Z-ATAD-fmk, Z-LEHD-fmk, and Z-DEVD-fmk, inhibitors for casp4, casp12, casp9, and casp3, respectively) for 2 h significantly diminished the RSV-induced apoptosis shown by annexin-V positive cells (Fig. 6b). To investigate the possible proapoptotic signal pathway, NPC cells pretreated with casp12, casp9 or casp3 inhibitors for 2 h prior to exposure to RSV for 24 h. The cell lysates were subjected to

Western blotting to investigate the levels of casp3/cleaved casp3 and PARP/cleaved PARP expression. Figure 6c indicates suppression of casp12, casp9 or casp3 activity decreased the levels of RSV-mediated cleaved PARP and cleaved casp3 expression. These results suggested the involvement of the RSV-mediated pro-apoptotic signaling pathway.

To investigate the possible role of casp12 and/or casp4 in the initiation of the RSV-mediated pro-apoptotic pathway, NPC cells pre-treated with Z-LEVD-fmk and Z-ATAD-fmk for 2 h prior to incubation with RSV for 24 h and the cell lysates were subjected to the apoptotic molecules by Western blotting. Figure 7a indicates that pretreatment with casp4/casp12 inhibitors markedly decreased the cleavage of casp9 and/or casp3 originally induced by RSV in a dose-dependent manner. Further, the

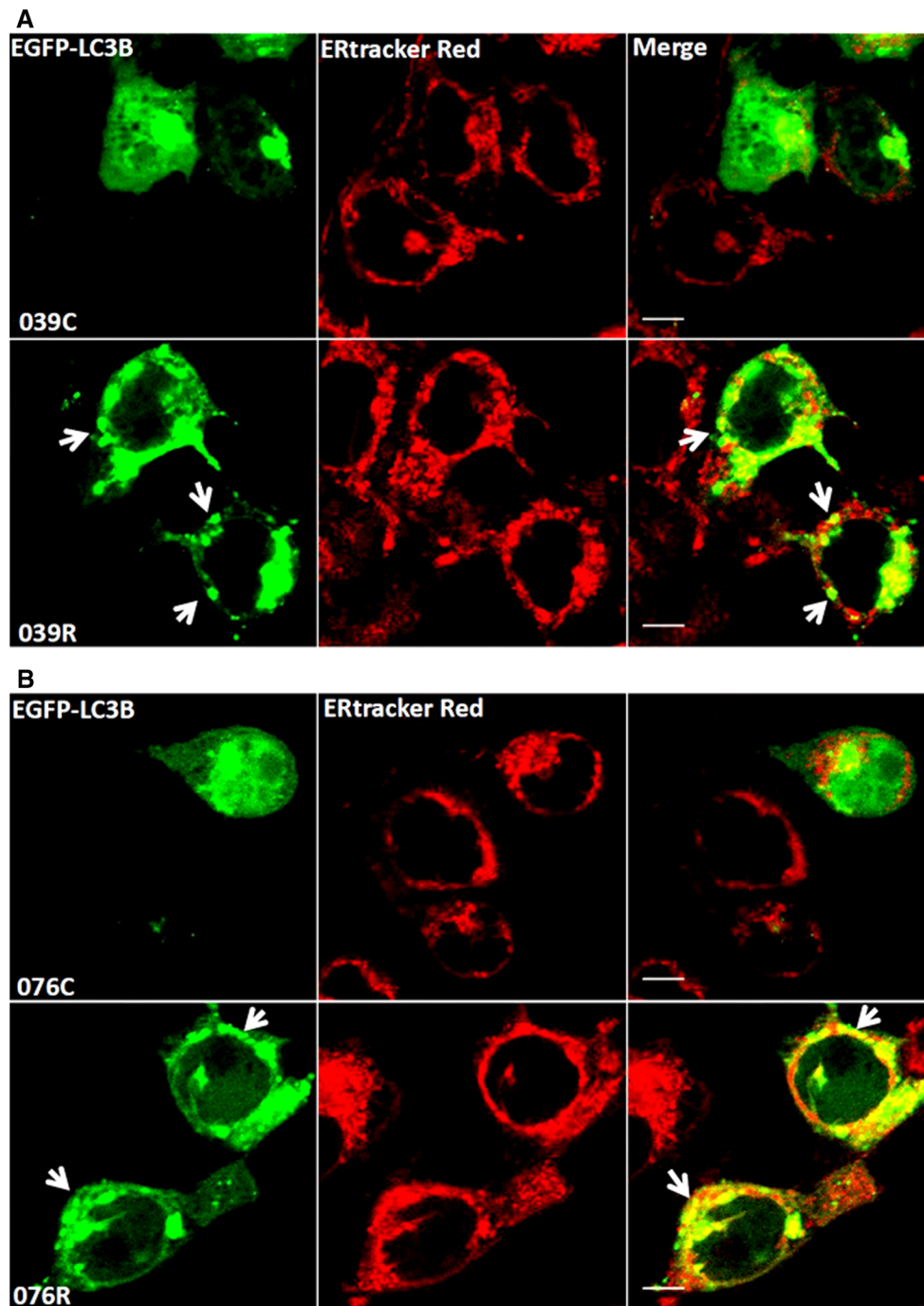


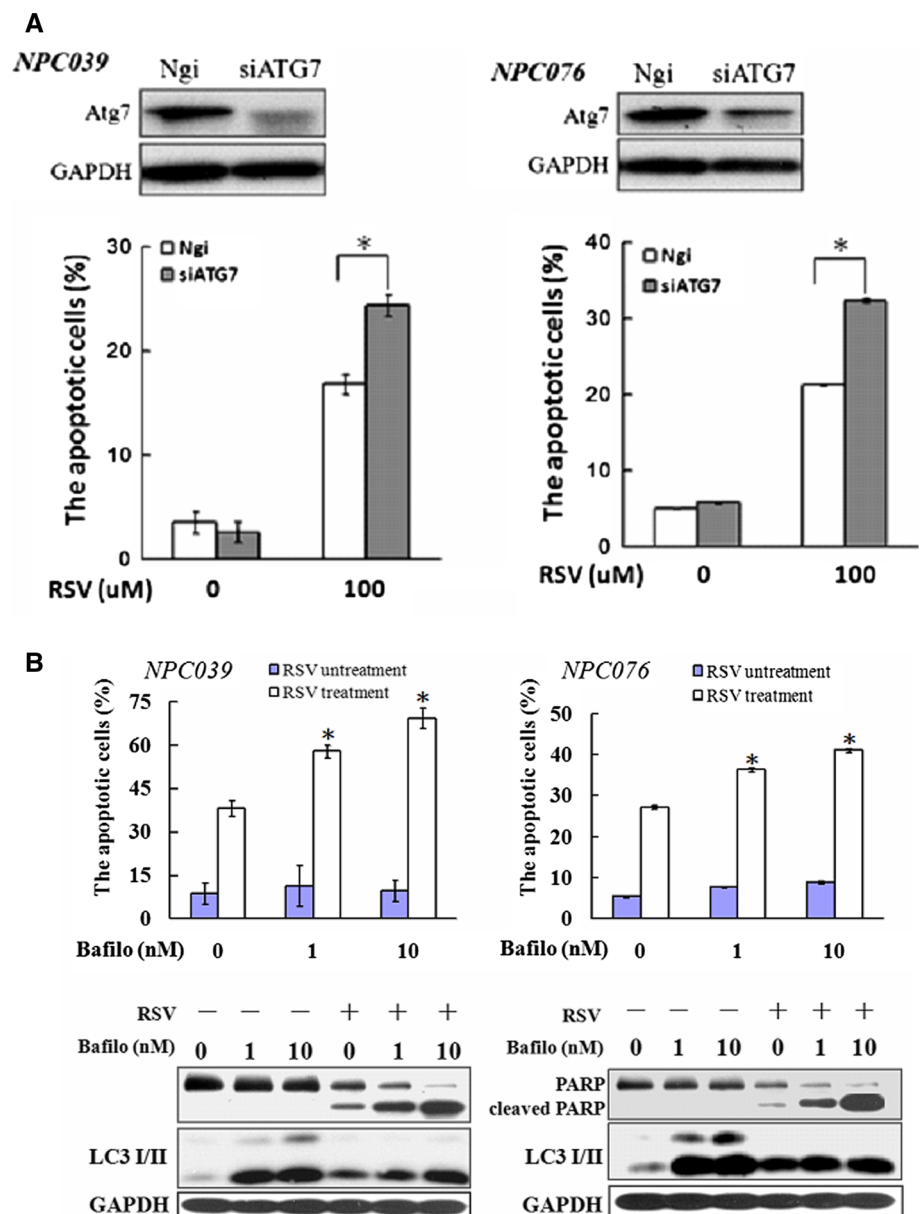
**Fig. 3** Co-localization of GFP-LC3 with ER Tracker Red. NPC cells were treated with RSV for 7 h prior to ectopic expression of EGFP-LC3 plasmid for 24 h, and then the cells were co-incubated with ER Tracker Red for 30 min. The images were collected under confocal fluorescence microscopy. The formation of EGFP-LC3-labeled

specificity of the casp4/casp12 in the initiation of the RSV-mediated pro-apoptotic pathway was assessed by siRNA transfection. Targeting silencing of casp12 or casp4 by siRNA for 24 h prior to incubation of RSV for 24 h, the cell apoptosis was investigated by annexin V-positive stained cells and the cell lysate was subjected to Western

puncta structures was observed in cells exposed to RSV (*white arrows*). **a** NPC-TW039. **b** NPC-TW076. The *first columns* for **a** and **b** were controls. The *second column* for **a** and **b** were NPC cells treated with RSV for 7 h

blotting. Figure 7b indicates casp12 expression was effectively decreased after siRNA transfection in NPC076 cells, but that was not significantly shown in NPC039 cells. This might be caused by a lower basal level of casp12 expression in RSV-untreated NPC039 cells. However, targeted silencing of casp12 effectively decreased the level of

**Fig. 4** Suppression of autophagosome maturation enhanced the RSV-mediated cell death. **a** NPC cells were transfected with negative control siRNA (Ngi), ATG7 siRNA for 24 h followed by exposure to RSV (100  $\mu$ M) for 24 h. NPC cells were stained with annexin V-cy5 and PI and then the apoptotic cells were assayed by flow cytometry (*upper panel*). The cell lysates were subjected to Western blotting for investigating ATG protein and GAPDH was used as a loading control. **b** NPC cells were pre-treated with bafilomycin A1 (1 or 10 nM) for 2 h prior to incubation with or without RSV (100  $\mu$ M) for 24 h. The cell apoptosis was determined by staining with annexin V/cy5-PI and analyzed by flow cytometry (*left panel*). Western blotting of the cell lysates was used to detect the levels of PARP/cleaved PARP and LC3 I/II. GAPDH was shown as a loading control. The blots shown represent the pattern found in three independent experiments. \* $p < 0.05$  (RSV and bafilomycin-cotreated cells compared with only RSV-treated cells)



RSV-induced casp12 expression and decreased the susceptibility of the cells to RSV-mediated cell death shown by decreased PARP cleavage and annexin-V positive cells (lower panel of Fig. 7b). Interestingly, targeted silencing of casp4 did not show any significant effect on RSV-mediated cell death shown by annexin-V positive cells (Fig. 7c). The data confirmed the inducible casp12 is a target of RSV in killing of NPC cells.

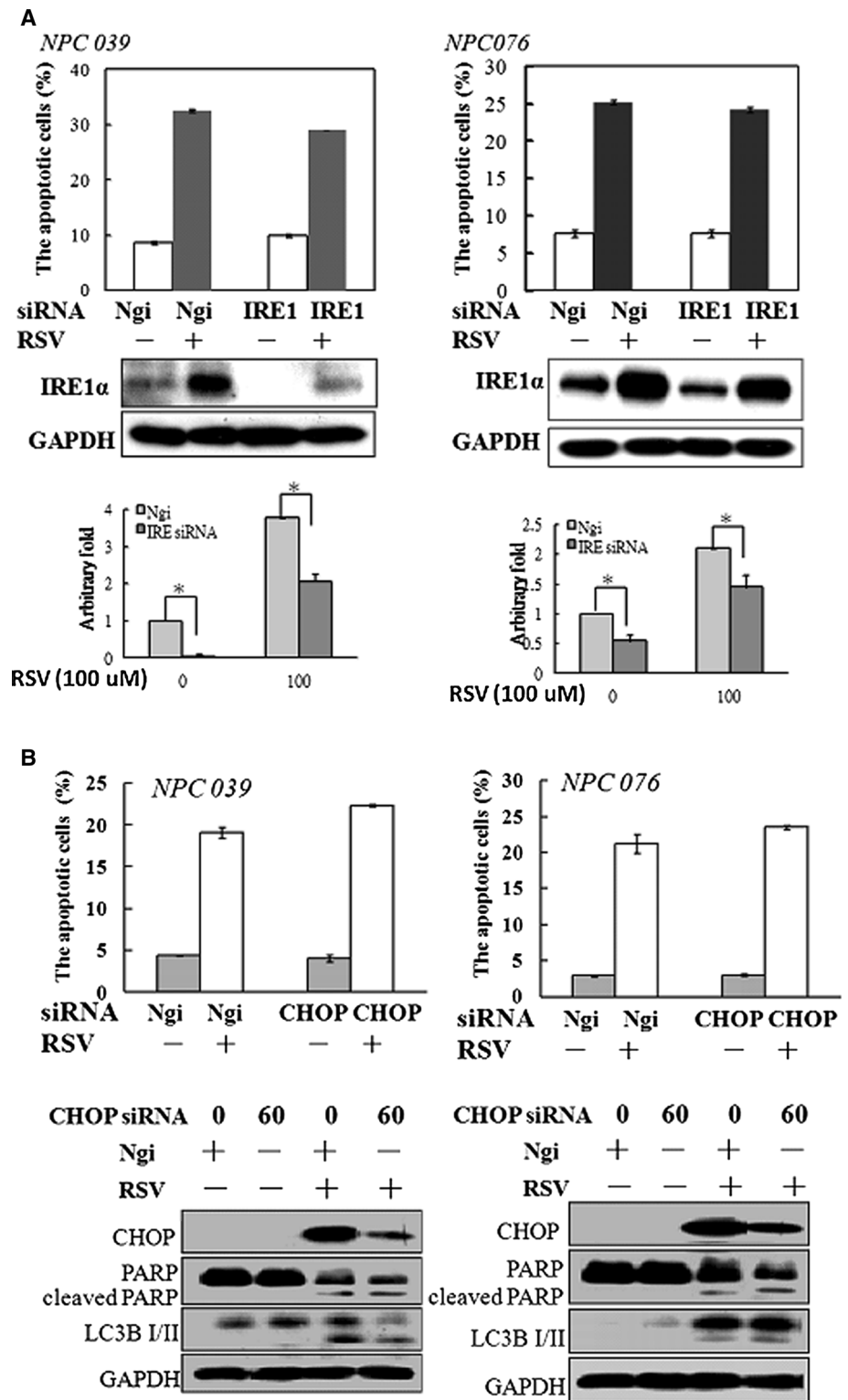
Suppression of de novo ceramide synthesis can counteract the biological effects of RSV

RSV has been shown to induce an increase of ceramide generation via activation of SPT to result in apoptosis [21]. Among the variety of ceramide species, C16 ceramide was

shown to be dominantly expressed in cancer cells. To investigate the effect of RSV on C16 ceramide accumulation, the lipids of NPC cells were extracted and analyzed by UPLC–MS/MS system. As shown in Fig. 8a, the relative percentage of C16 ceramide markedly increased in RSV-treated cells compared with that in control group cells. At concentrations of 50 and 100  $\mu$ M, RSV increased C16 ceramide by 2 and 2.7 fold in NPC039 cells and by 7.4 and 8.6 fold in NPC076 cells, respectively, suggesting abnormal accumulation of ceramide. Abnormal lipid accumulation is shown to induce ER expansion [28]. De novo ceramide biosynthesis begins with the condensation of serine and palmitoyl-CoA catalysed by the serine palmitoyltransferase complex (SPT), which is also an ER resident [21]. To identify the biological effects of ceramide on RSV-mediated



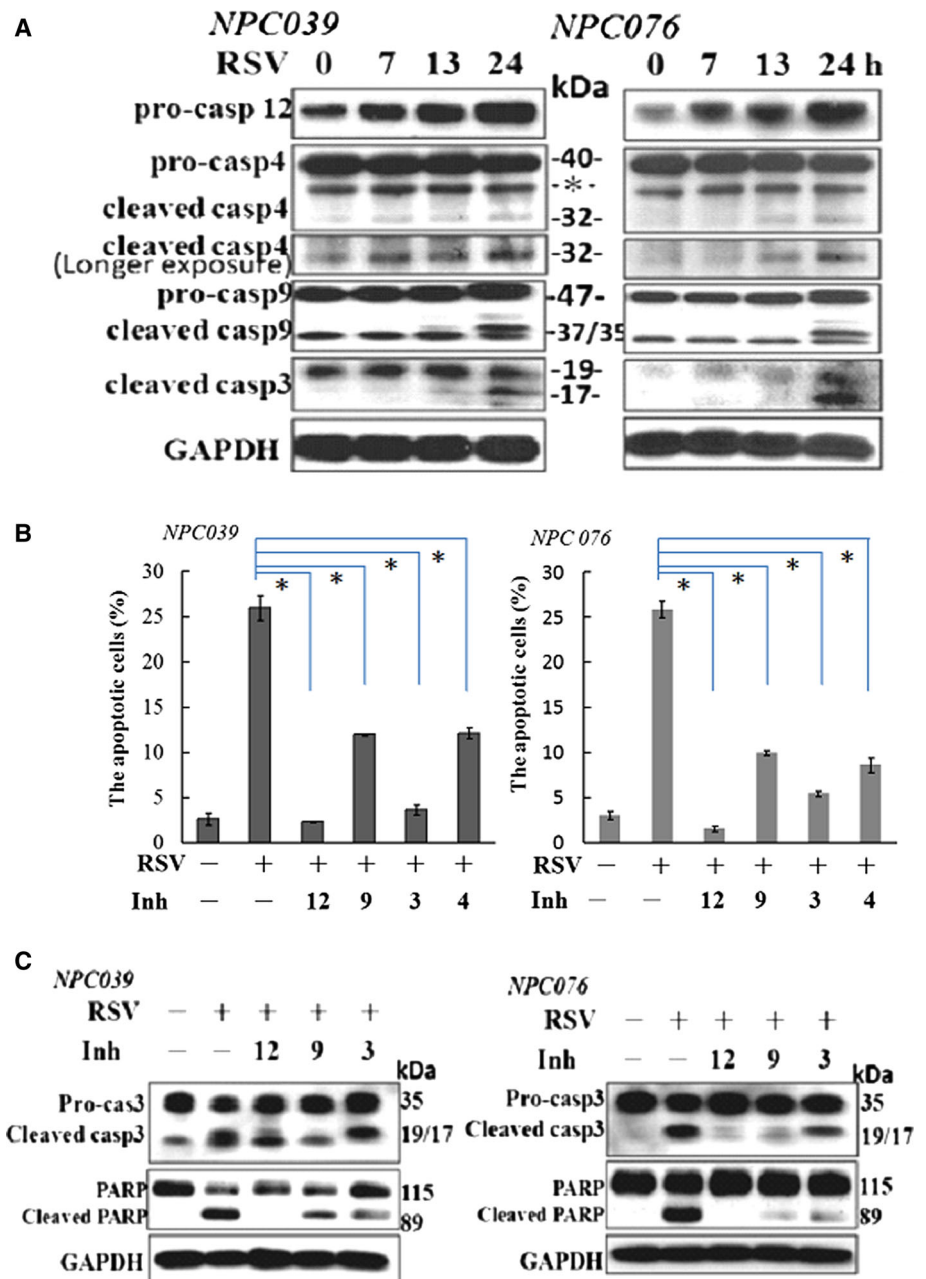
**Fig. 5** Upregulation of IRE1/CHOP was not involved in RSV-mediated cell apoptosis. NPC cells were transfected with negative control siRNA (Ngi), IRE1 siRNA (a), or CHOP siRNA (b) for 24 h, and then treatment with or without RSV (100  $\mu$ M) for 24 h. The NPC cells were stained with annexin V-cy5 and PI and then the apoptotic cells were assayed by flow cytometry (*left panel*). The lysate was subjected to Western blotting to investigate IRE1, CHOP, PARP/cleaved PARP, or LC3 I/II as indicated. GAPDH was shown as a loading control. The blots shown represent a pattern from three independent experiments. The indicated protein expression of each group was normalized to that of GAPDH. The *histograms* represent fold changes relative to controls that were arbitrarily set at 1. \* $p < 0.05$  versus control group



ER stress, NPC cells incubated with RSV alone or in combination with SPT inhibitors, *L*-cycloserine (Cyc, 1 mM) or myriocin (Myr, 5  $\mu$ M) for 24 h. Western blotting was used to analyze the cell lysate and investigate the expressions of LC3 I/II, CHOP and PARP cleavage. As

shown in Fig. 8b, Cyc and Myr markedly reduced PARP cleavage, CHOP and LC3-II expression induced by RSV. Further, Cyc markedly counteracted the effect of RSV on the expression of casp4 and casp12 (Fig. 8c). Next, the treated NPC cells were fixed and sliced into 0.6  $\mu$ m sections,

**Fig. 6** RSV induced the casp4/casp12-mediated proapoptotic pathway. **a** RSV induced ER caspases-mediated cell death. NPC cells were treated with RSV (100  $\mu$ M) at the indicated periods. Cell lysates were subjected to investigation of the levels of casp12, casp4, casp9, and active casp3. **b** Specific ER caspase inhibitors inhibited RSV-induced cell death. NPC cells with or without pre-treatment with caspase inhibitors (Z-ATAD-fmk, Z-LEHD-fmk, Z-DEVD-fmk, and Z-LEVD-fmk, specific inhibitors of casp12, casp9, casp3, and casp4, respectively) were treated with RSV (100  $\mu$ M) for 24 h. Cell apoptosis was determined by annexin V/cy5-PI staining and analyzed by flow cytometry. *Asterisk* shows a nonspecific band for casp4 antibody. Longer exposure showed the presence of cleaved casp4 (32 kDa), which is marked as “longer exposure”. **c** The proapoptotic signaling pathway. NPC cells were treated with casp12, casp9, and casp3 inhibitors for 2 h prior to exposure to RSV for 24 h. The cell lysates were subjected to Western blotting to investigate the expression of PARP/cleaved PARP and/or casp3/cleaved casp3. GAPDH was shown as a loading control. Data shown represent three independent experiments



stained with toluidine blue and then observed under light microscopy. As shown in Fig. 8d, Cyc markedly decreased the level of ER dilation induced by RSV. The data indicated RSV-mediated ER expansion via abnormal accumulation of ceramide and suggested RSV-mediated ceramide has a role in the induction of events in ER stress.

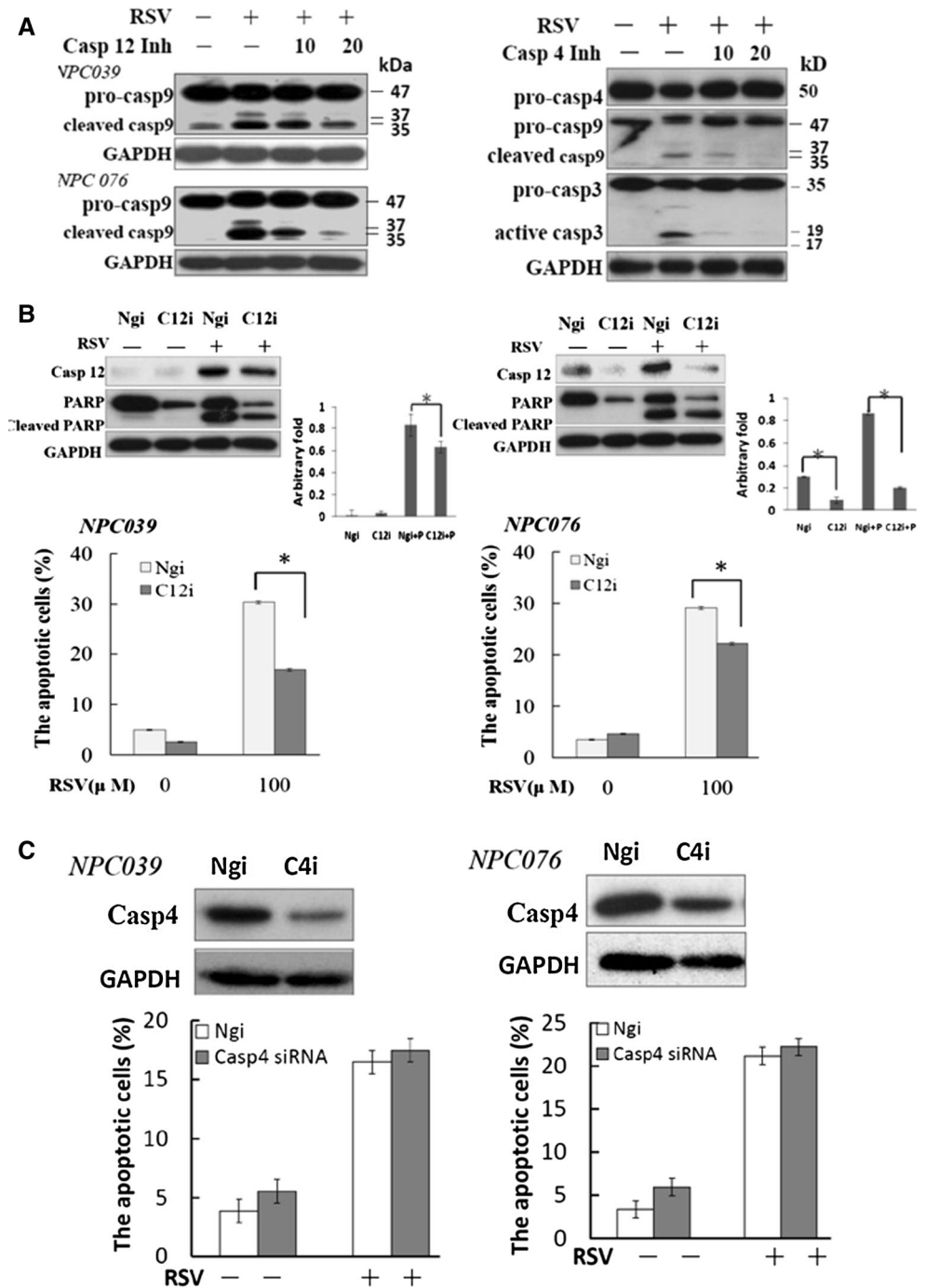
## Discussion

The importance of the UPR under oncogenic stress in cancer cells has inspired great interest in exploring therapeutic potentials through targeting the UPR-induced

pathway. In this study, the mechanisms underlying RSV-mediated NPC cell apoptosis associated with ER stress and autophagy were investigated. We found that severe ER expansion and up-regulation of the ER-associated casp12 might contribute to RSV-mediated cell death. Interestingly, RSV might induce ER-phagy, and the lipidation of LC3 might be engaged in the dilation of ER. Under prolonged exposure to RSV, the two specific ER resident casp4 and casp12 might be activated to initiate the onset of cell death via the casp9/casp3 pathway. Interestingly, we found that knockdown of casp12, but not casp4, decreased the RSV-mediated cell death. SPT inhibitors were able to counteract the RSV-induced biological events. Thus, this study

**Fig. 7** Targeted silencing of casp12 by siRNA decreased the antitumor effect of RSV.

**a** Casp12/casp4-mediated cell death was via activation of casp9 pathway. NPC cells were pre-treated with casp12 inhibitor (Z-ATAD-fmk, 10–20  $\mu$ M) or casp4 inhibitor (Z-LEVD-fmk, 10–20  $\mu$ M) for 2 h prior to exposure to RSV (100  $\mu$ M) for 24 h. The cell lysates of both treated cells and control cells were subjected to Western blotting for detection of casp9/cleaved casp9 or casp3/cleaved casp3 levels. **b**, **c** NPC cells were transfected with casp12 siRNA (**b**) or casp4 siRNA (**c**) for 24 h prior to treatment with RSV for another 24 h. NPC cells were stained with annexin V-cy5 and PI, and the apoptotic cells were assayed by flow cytometry. The cell lysates were subjected to Western blotting to detect the expression of casp12 or casp4 and/or PARP/cleaved PARP. GAPDH was shown as a loading control. The blots shown represent three independent experiments. \* $p < 0.05$  (casp12 or casp4 siRNA and RSV-treated cells compared with only RSV-treated cells)

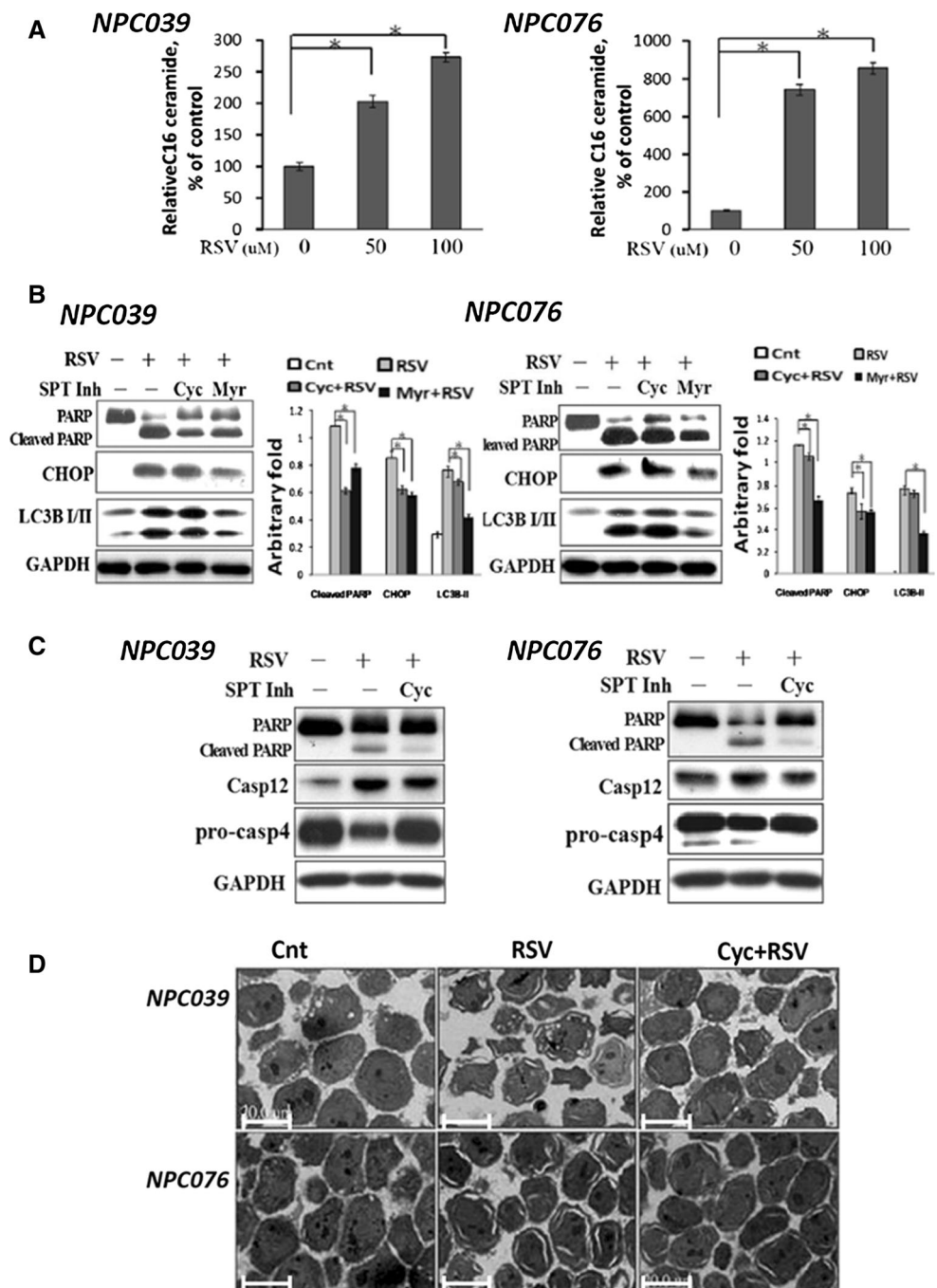


revealed the ER expansion and upregulation of ER casp12 might be implicated in the RSV's effect.

Changes in the ER that interfere with the proper maturation of secreted proteins initiates a coordinated adaptive program called the unfolded protein response (UPR) to avoid cell damage [4]. It has been shown that activation of the UPR in yeast induces ER-phagy, a selective autophagy of the ER [6]. ER-phagy involves the generation of autophagosomes that selectively include ER membranes [29]. In this study, RSV induced increased level of LC3-II

accompanied with UPR expression and ER dilation in a time-dependent manner (Figs. 1, 2). After a 7 h treatment, RSV simultaneously induced the co-localization of ER-tracker Red dye-stained EGFP-LC3 puncta (Fig. 3) and the crescent-like vacuoles containing multi-lamellar membrane structure. The data suggests the possible role of LC3-II engaged in the lipid source of expanded ER membrane and/or the ER-derived membrane source for autophagosome formation (ER-phagy). It might represent an important degradative function of the UPR that helps in the onset of

**Fig. 8** Suppression of ceramide biosynthesis might counteract the effects of RSV. **a** RSV induced ceramide accumulation. NPC cells were incubated with RSV at indicated concentrations for 24 h. Lipid was extracted and C16 ceramide investigated by UPLC–MS/MS system shown in “Materials and methods”. The relative percentage of ceramide in RSV-treated NPC cell was compared with that of RSV-untreated NPC cell prior to normalization to the total cellular protein ( $N = 3$ ,  $*p < 0.05$ ). **b** NPC cells were treated with RSV (100  $\mu\text{M}$ ) for 24 h after pre-treatment with or without the SPT inhibitors (1 mM L-cycloserine and 5  $\mu\text{M}$  myriocin) for 2 h. The lysate was subjected to Western blotting to investigate the levels of CHOP, PARP/cleaved PARP, and LC3 I/II. **c** RSV-mediated ceramide induced activation of casp4 and casp12. NPC cells were pre-treated with or without the SPT inhibitor (0.5–1 mM L-cycloserine) for 2 h prior to incubation with RSV (100  $\mu\text{M}$ ) for 24 h. The lysate was subjected to Western blotting to detect the levels of casp12 and casp4. GAPDH was shown as a loading control. The blots shown are representative of a pattern from three independent experiments. **d** The dilation of ER was assayed after pretreatment with SPT inhibitor (Cyc) for 2 h and then incubation with RSV for 24 h, the cells were fixed, sliced into 0.6  $\mu\text{m}$  sections and then stained with toluidine blue for observation with light microscopy (LM)



ER homeostatic control. The presence of debris or multi-lamella membrane structures in the crescent-like vacuoles similar to autophagosomes, indicates that RSV induced catabolic reaction via the non-canonical autophagy. Whether the role of crescent vacuoles is implicated with the ER-associated autophagosome remains to be investigated. After a 24 h treatment, TEM images showed that RSV induced a massive accumulation of ER expansion. The enlarged ER cisternae containing the digested debris were present in the subcellular compartment (Fig. 1), suggesting

a catabolic action in the compartment of dilated ER that might be fused with lysosomes.

Accumulating data indicate that ER stress is a potent trigger of autophagy. RSV induced LC3-II in a time-dependent manner accompanied by ER stress as shown by increased expression of the UPR signaling molecules ATF6, IRE1, p-PERK. These molecules suggest that ER stress induces autophagy. LC3-II formation is the most commonly used marker of autophagy in most studies; however, the amount of LC3 at a certain time point does

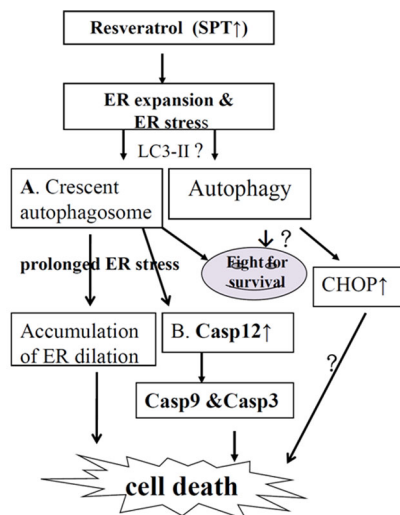
not indicate autophagic flux and it is important to measure the amount of LC3-II delivered to lysosomes by comparing LC3-II levels in relation to E64d/pepstatinA, which inhibit lysosome proteases, or bafilomycin A1, which inhibits the fusion of autophagosome and lysosome [27, 30]. Lysosomal turnover of endogenous LC3 (autophagic flux) is a more reliable indicator of autophagic activity than measurements of autophagosome numbers [27]. In this study, bafilomycin A1 effectively inhibit RSV-induced autophagic flux evidenced by the accumulation of LC3-II. Inhibition of autophagy either at an early (elongation) stage by ATG7 siRNA or at a late (fusion) stage by bafilomycin A1 caused increased cell death mediated by RSV, which implicates the importance of RSV in modulating NPC cell death by inducing an alternative autophagic pathway.

ER has evolved the UPR that modulates several transcription factors (e.g., ATF6, XBP1 and CHOP) in an attempt to adapt for survival or otherwise undergo apoptosis facing prolonged UPR. This study found prolonged exposure or severe ER stress led to the upregulation of CHOP, potentially a downstream molecule of the UPR. CHOP, a member of the CCAAT/enhancer-binding protein family, participates in ER-mediated apoptosis in carcinoma cells [31]. Treatment with RSV increased ER stress, up regulating the UPR and inducing of CHOP in NPC cells. Interestingly, targeted silencing of the UPR molecule IRE1 or CHOP by siRNA did not significantly alter RSV-induced apoptosis [8]. NPC cancer cells might adapt to ER stress and evade stress-induced apoptotic pathways by differentially activating the UPR branches [2]. Thus, the potential mechanisms underlying the proapoptotic molecules in carcinoma cells were further investigated. It has been shown that casp12 is specifically activated by ER stress, inducing disruption of ER calcium homeostasis and accumulation of excess proteins in ER [11]. Human casp4, one of the closest paralogs of rodent casp-12, can perform the functions normally ascribed to rodent casp12 in the context of ER stress [9]. Casp4 in human neuroblastoma cells is also shown to partially involved in cell death caused by the ER stress inducers thapsigargin and amyloid  $\beta$ -peptide (A $\beta$ P) [9]. This study showed that the activation of casp4 and up-regulation of casp12, two ER residents, are involved in the onset of RSV-mediated apoptosis. The activity of casp4/casp12 was confirmed by pretreatment with their inhibitors. Intriguingly, knock-down of casp12, but not casp4, diminished the RSV-mediated apoptosis, confirming the role of casp12 in the regulation of ER stress-mediated cell death. However, knock-down of casp4 in HeLa cells had little effect on apoptosis induced by ER stress, implying that the relevance of this protease to ER stress is tissue-specific [9]. Activated casp12 causes the cleavage of casp9, which further cleaves and activates casp3 to result in cell apoptosis [12, 32]. Human casp12 is

shown to contain a premature stop codon [13]. Recent studies have shown that casp12 is present in some cancer cells and in the proximal tubule of human kidneys under a particular pathologic condition [14–16], suggesting the possibility that casp12 is tissue-specifically distributed. These studies together suggest that ER stress-mediated cell death via activation of the casp12 pathway in epithelial or carcinoma cells. The regulation mechanism of casp12 in NPC cells is further under investigation in our laboratory.

The sphingolipid ceramide is one component for the plasma membrane that is generated through a major pathway of de novo biosynthesis by serine palmitoltransferase (SPT) [33]. It has been recognized as an important secondary messenger implicated in regulating signaling pathways, especially for apoptosis [33]. ER functions as a protein-folding compartment and is also the major site for lipid synthesis, including ceramide biosynthesis. Abnormal synthesis of phospholipids in the ER has been shown to disrupt the morphology of the ER as well as the induction of fatty acid-induced ER stress [21]. Palmitic acid is shown to mediate lipid composition and localization to cause ER expansion and consequently result in ER stress [28]. RSV induces growth inhibition/apoptosis in breast cancer in concomitance with a consistent accumulation of endogenous ceramide via the key enzyme of de novo ceramide biosynthetic pathway [21]. Consistent with these studies, RSV also induced C16 ceramide accumulation in NPC cells in a dose-dependent manner. Two SPT inhibitors (*L*-cycloserine and myriocin) decreased the activation of casp4/casp12, as well as the levels of CHOP and LC3-II to suggest that accumulated ceramide mediates the effects of RSV. Interestingly, the SPT inhibitor decreased the level of RSV-mediated ER expansion and only the SPT inhibitors could rescue RSV-treated cells from apoptosis [21]. This study clearly indicated the effect of ceramide accumulation on the ER stress induction and inhibition of de novo ceramide biosynthesis would act against the biological effects of RSV. Thus, together with our data, it might suggest the effect of RSV on ceramide biosynthesis is not cell type specific.

RSV, a naturally occurring dietary compound with chemopreventive properties has been reported to trigger apoptosis in a variety of cancer cell types. It induces apoptosis of human NPC cells via the activation of multiple apoptotic pathways [34]. In our previous study, it has shown that RSV induced  $\Delta$ NP63-dependent apoptosis in a dose-dependent manner [35]. RSV (12–100  $\mu$ M) induces dose-dependent growth suppression, cell cycle arrest in the S phase and caspase-dependent apoptosis. The antitumor potential of RSV depends, in part, on its absorption, metabolism, and bioavailability [36]. Resveratrol glucuronides and sulfates are the most frequently reported phase II metabolites, implicating the bioavailability of RSV [37], whereas it has reported that resveratrol monosulfate is the major metabolite in culture cancer



**A model proposed for RSV-induced cell apoptosis**

**Fig. 9** A model proposed for RSV-induced cell apoptosis. ER dilation might be the major sources of crescent autophagosomes (a). Casp-12 might be a cause for ER stress-mediated apoptosis (b)

cells [38]. The RSV presented in the culture medium (in vitro) is relatively stability than in vivo [39]. It has been shown that RSV is the bioactive form in medulloblastoma cells and fibroblast cells [37, 38]. To convincingly show the ability of RSV to induce apoptosis in NPC cells, we chose doses around 50–100  $\mu\text{M}$  [35]. Doses required for RSV to induce apoptosis were higher than those that induced growth inhibition and cell cycle arrest, often in the 100–200  $\mu\text{M}$  range. Determination of the bioactive form or forms of RSV in individual cell and cancer types is a fundamental issue for the successful application of RSV in clinical therapy. The results of this study merit further clinical evaluation of RSV as a potential NPC cancer chemopreventive agent.

This study identified ER stress mediated cell death induced by RSV in regulating the UPR events, ER caspases and non-canonical autophagy. RSV induced severe ER stress and ER expansion that exhausted its protective features which triggered its ER-residing pro-apoptotic modules, casp4 and casp12 (Fig. 9). Importantly, this study indicated the role of casp12 in regulating the ER stress-mediated cell death in human carcinoma cells. Thus, this study might offer an advantage for the agents that target the ER to achieve specificity in cancer therapy.

**Acknowledgments** This work was supported by Chang Gung Memorial Hospital & Chang Gung University. Contract Grant Number: CMRPD 1B0231, CMRPD 5C0011 and EMRPD 1C0271.

## References

1. Xu CY, Bailly-Maitre B, Reed JC (2005) Endoplasmic reticulum stress: cell life and death decisions. *J Clin Invest* 115:2656–2664

- Schönthal AH (2013) Pharmacological targeting of endoplasmic reticulum stress signaling in cancer. *Biochem Pharmacol* 85: 653–666
- Li XM, Zhang KH, Li ZH (2011) Unfolded protein response in cancer: the physician's perspective. *J Hematol Oncol* 4:8. doi:10.1186/1756-8722-4-8
- Verfaillie T, Salazar M, Velasco G, Agostinis P (2010) Linking ER Stress to autophagy: potential implications for cancer therapy. *Int J Cell Biol*. doi:10.1155/2010/930509
- Walker D (2010) Autophagy: a new link in the chain. *Nat Rev Mol Cell Biol* 11:604–605
- Bernales S, Schuck S, Walter P (2007) ER-phagy: selective autophagy of the endoplasmic reticulum. *Autophagy* 3:285–287
- Codogno P, Mehrpour M, Proikas-Cezanne T (2011) Canonical and non-canonical autophagy: variations on a common theme of self-eating? *Nat Rev Mol Cell Biol* 13:7–12
- Jing G, Wang JJ, Zhang SX (2012) ER stress and apoptosis: a new mechanism for retinal cell death. *Exp Diabetes Res*. doi:10.1155/2012/589589
- Hitomi J, Katayama T, Eguch Y, Kudo T, Taniguchi M, Koyama Y, Manabe T, Yamagishi S, Bando Y, Imaizumi K, Tsujimoto Y, Tohyama M (2004) Involvement of caspase-4 in endoplasmic reticulum stress-induced apoptosis and A $\beta$ -induced cell death. *J Cell Biol* 165:347–356. doi:10.1083/jcb.200310015
- Nakagawa T, Zhu H, Morishima N, Li E, Xu J, Yuan BA, Yankner J (2000) Caspase-12 mediates endoplasmic-reticulum-specific apoptosis and cytotoxicity by amyloid- $\beta$ . *Nature* 403:98–103
- Yoneda T, Imaizumi K, Oono K, Yui D, Gom F, Katayama T, Tohyama M (2001) Activation of caspase-12, an endoplasmic reticulum (ER) resident caspase, through tumor necrosis factor receptor-associated factor 2-dependent mechanism in response to the ER stress. *J Biol Chem* 276:13935–13940
- Morishima N, Nakanishi K, Takenouchi H, Shibata T, Yasuhiko Y (2002) An endoplasmic reticulum stress-specific caspase cascade in apoptosis: cytochrome C-independent activation of caspase-9 by caspase-12. *J Biol Chem* 277:34287–34294
- Saleh M, Vaillancourt JP, Graham RK, Huyck M, Srinivasula SM, Alnemri ES, Steinberg MH, Nolan V, Baldwin CT, Hotchkiss RS, Buchman TG, Zehnbauser BA, Hayden MR, Farrer LA, Roy S, Nicholson DW (2004) Differential modulation of endotoxin responsiveness by human caspase-12 polymorphisms. *Nature* 429:75–79
- Cheng CY, Su CC (2010) Tanshinone IIA inhibits Hep-J5 cells by increasing calreticulin, caspase 12 and GADD153 protein expression. *Int J Mol Med* 26:379–385
- Cheng CY, Lin YH, Su CC (2010) Curcumin inhibits the proliferation of human hepatocellular carcinoma J5 cells by inducing endoplasmic reticulum stress and mitochondrial dysfunction. *Int J Mol Med* 26:673–678
- Chauhan D, Singh AV, Ciccarelli B, Richardson PG, Palladino MA, Anderson KC (2010) Combination of novel proteasome inhibitor NPI-0052 and lenalidomide trigger in vitro and in vivo synergistic cytotoxicity in multiple myeloma. *Blood* 115:834–845
- Brezniceanu ML, Lau CJ, Godin N, Chénier I, Duclos A, Éthier J, Filep JG, Ingelfinger JR, Zhang SL, Chan JS (2010) Reactive oxygen species promote caspase-12 expression and tubular apoptosis in diabetic nephropathy. *J Am Soc Nephrol* 21:943–954
- Wang FM, Galson DL, Roodman GD, Ouyang H (2011) Resveratrol triggers the pro-apoptotic endoplasmic reticulum stress response and represses pro-survival XBPI signaling in human multiple myeloma cells. *Exp Hematol* 39:999–1006
- Pattingre S, Bauvy C, Levade T, Levine B, Codogno P (2009) Ceramide-induced autophagy: to junk or to protect cells? *Autophagy* 5:558–560
- Mauthe M, Jacob A, Freiberger S, Hentschel K, Stierhof YD, Codogno P, Proikas-Cezanne T (2011) Resveratrol-mediated

- autophagy requires WIPI-1-regulated LC3 lipidation in the absence of induced phagophore formation. *Autophagy* 7:1448–1461
21. Scarlatti F, Scarlatti F, Sala G, Somenzi G, Signorelli P, Sacchi N, Ghidoni R (2003) Resveratrol induces growth inhibition and apoptosis in metastatic breast cancer cells via de novo ceramide signaling. *FASEB J* 17:2339–2341
  22. Lin CT, Wong CI, Chan WY, Tzung KW, Ho JK, Hsu MM, Chuang SM (1990) Establishment and characterization of two nasopharyngeal carcinoma cell lines. *Lab Invest* 62:713–724
  23. Chow SE, Chen YW, Liang CA, Huang YK, Wang JS (2012) Wogonin induces cross-regulation between autophagy and apoptosis via a variety of Akt pathway in human nasopharyngeal carcinoma cells. *J Cell Biochem* 113:3476–3485
  24. Chow SE, Chang YL, Chuang SF, Wang JS (2011) Wogonin induced apoptosis in human nasopharyngeal carcinoma cells by targeting GSK-3 $\beta$  and  $\Delta$ Np63. *Cancer Chemother Pharmacol* 68:835–845
  25. Zhang K, Haynes T-AS, Filippova M, Filippov V, Duerksen-Hughes PJ (2011) Quantification of ceramide levels in mammalian cells by high performance liquid chromatography coupled to tandem mass spectrometry with multiple-reaction-monitoring mode (HPLC–MS/MS–MRM). *Anal Method* 3:1193–1197
  26. Mizushima N, Ohsumi Y, Yoshimori T (2002) Autophagosome formation in mammalian cells. *Cell Struct Funct* 27:421–429
  27. Mizushima N, Yoshimori T, Levine B (2010) Methods in mammalian autophagy research. *Cell* 140:313–326
  28. Peng G, Li L, Liu Y, Pu J, Zhang S, Yu J, Zhao J, Liu P (2011) Oleate blocks palmitate-induced abnormal lipid distribution, endoplasmic reticulum expansion and stress, and insulin resistance in skeletal muscle. *Endocrinol* 152:2206–2218
  29. Bernales S, McDonald KL, Walter P (2006) Autophagy counterbalances endoplasmic reticulum expansion during the unfolded protein response. *PLoS Biol* 4:e423. doi:10.1371/journal.pbio.0040423
  30. Tanida I, Minematsu-Ikeguchi N, Ueno T, Kominami E (2005) Lysosomal turnover, but not a cellular level, of endogenous LC3 is a marker for autophagy. *Autophagy* 1:84–91
  31. Yamaguchi H, Wang HG (2004) CHOP is involved in endoplasmic reticulum stress-induced apoptosis by enhancing DR5 expression in human carcinoma cells. *J Biol Chem* 279:45495–45502
  32. Kerbirou M, Teng L, Benz N, Trouvé P, Férec C (2009) The calpain, caspase 12, caspase 3 cascade leading to apoptosis is altered in F508del-CFTR expressing cells. *PLoS One* 4:e8436. doi:10.1371/journal.pone.0008436
  33. Pettus BJ, Chalfant CE, Hannun YA (2002) Ceramide in apoptosis: an overview and current perspectives. *Biochim Biophys Acta* 1585:114–125
  34. Huang T-T, Lin H-C, Chen C-C, Lu C-C, Wei C-F, Wu T-S, Liu F-G, Lai H-C (2011) Resveratrol induces apoptosis of human nasopharyngeal carcinoma cells via activation of multiple apoptotic pathways. *J Cell Physiol* 226:720–728
  35. Chow SE, Wang JS, Chuang SF, Chang YL, Chu WK, Chen WS, Chen YW (2010) Resveratrol-induced p53-independent apoptosis of human nasopharyngeal carcinoma cells is correlated with the downregulation of  $\Delta$ Np63. *Cancer Gene Ther* 17:872–882
  36. Cottart C, Nivet-Antoine V, Laguillier-Morizot C, Beaudeau J (2010) Resveratrol bioavailability and toxicity in humans. *Mol Nutr Food Res* 54:7–16
  37. Shu X-H, Li H, Sun Z, Wu M-L, Ma J-X, Wang J-M, Wang Q, Sun Y, Fu Y-S, Chen X-Y, Kong Q-Y, Liu J (2010) Identification of metabolic pattern and bioactive form of resveratrol in human medulloblastoma cells. *Biochem Pharmacol* 79:1516–1525
  38. Giovannelli L, Pitozzi V, Jacomelli M, Mulinacci N, Laurenzana A, Dolara P, Mocali A (2011) Protective effects of resveratrol against senescence-associated changes in cultured human fibroblasts. *J Gerontol A Biol Sci Med Sci* 66A:9–18
  39. Florey O, Kim SE, Sandoval CP, Haynes CM, Overholtzer M (2011) Autophagy machinery mediates macroendocytic processing and entotic cell death by targeting single membranes. *Nat Cell Biol* 13:1335–1343